The Plant Journal (2004) **40**, 428–438 doi: 10.1111/j.1365-313X.2004.02219.x

TECHNICAL ADVANCE

Visualization of protein interactions in living plant cells using bimolecular fluorescence complementation

Michael Walter[1], Christina Chaban[2], Katia Schütze[2], Oliver Batistic[1], Katrin Weckermann[3], Christian Näke[2], Dragica Blazevic[1], Christopher Grefen[2], Karin Schumacher[3], Claudia Oecking[3], Klaus Harter[2,*] and Jörg Kudla[1,*]

[1]*Institut für Botanik und Botanischer Garten, Molekulare Entwicklungsbiologie der Pflanzen, Universität Münster, Schlossplatz 4, 48149 Münster, Germany,*

[2]*Botanisches Institut, Universität zu Köln, Gyrhofstr. 15, 50931 Köln, Germany, and*

[3]*ZMBP, Pflanzenphysiologie, Universität Tübingen, Auf der Morgenstelle 1, 72076 Tübingen, Germany*

Received 24 June 2004; revised 6 August 2004; accepted 12 August 2004.

[*]For correspondence (fax +49 251 83 23311; e-mail jkudla@uni-muenster.de: fax +49 221 470 7765; e-mail klaus.harter@uni-koeln.de).

Summary

Dynamic networks of protein–protein interactions regulate numerous cellular processes and determine the ability to respond appropriately to environmental stimuli. However, the investigation of protein complex formation in living plant cells by methods such as fluorescence resonance energy transfer has remained experimentally difficult, time consuming and requires sophisticated technical equipment. Here, we report the implementation of a bimolecular fluorescence complementation (BiFC) technique for visualization of protein–protein interactions in plant cells. This approach relies on the formation of a fluorescent complex by two non-fluorescent fragments of the yellow fluorescent protein brought together by association of interacting proteins fused to these fragments (Hu *et al.*, 2002). To enable BiFC analyses in plant cells, we generated different complementary sets of expression vectors, which enable protein interaction studies in transiently or stably transformed cells. These vectors were used to investigate and visualize homodimerization of the basic leucine zipper (bZIP) transcription factor bZIP63 and the zinc finger protein lesion simulating disease 1 (LSD1) from *Arabidopsis* as well as the dimer formation of the tobacco 14-3-3 protein T14-3c. The interaction analyses of these model proteins established the feasibility of BiFC analyses for efficient visualization of structurally distinct proteins in different cellular compartments. Our investigations revealed a remarkable signal fluorescence intensity of interacting protein complexes as well as a high reproducibility and technical simplicity of the method in different plant systems. Consequently, the BiFC approach should significantly facilitate the visualization of the subcellular sites of protein interactions under conditions that closely reflect the normal physiological environment.

Keywords: bimolecular fluorescence complementation, protein–protein interaction, intracellular localization, bZIP transcription factor, 14-3-3 proteins, LSD1.

Introduction

The regulation and execution of biological processes requires specific interactions of numerous proteins. Tightly regulated protein interaction networks mediate cellular responses to environmental cues and direct the implementation of developmental programs. The selectivity of protein–protein interactions and their appropriate temporal and spatial regulation determine the developmental potential of the cell and its response to endogenous and exogenous signals. On the molecular level differential protein–protein interactions are thought to determine the operation of complex regulatory circuits and signal transduction systems.

The complete sequencing of an increasing number of eukaryotic genomes has provided a wealth of information about the number and complexity of protein functions

required to build up an organism. However, the regulation and interplays of these proteins remain to become explored in order to appreciate the molecular mechanisms of their action. Several methods have been developed to identify, examine and visualize protein interactions and protein complexes in living cells. Among them, the yeast two-hybrid system has significantly advanced the speed and extent of protein interaction studies. However, this system bears intrinsic limitations as for example systematic 'false-positive' and 'false-negative' interactions and, moreover, usually combines protein pairs in a heterologous environment (Field and Song, 1989; Stephens and Banting, 2000). The most widely used approach for the visualization of protein interactions in living cells is fluorescence resonance energy transfer (FRET) between spectral variants of the green fluorescence protein (GFP) fused to the associating proteins (Chen *et al.*, 2003; Periasamy, 2000). However, to enable observation and quantification of small alterations in fluorescence emission, the GFP fluorophores have to join in close spatial proximity and the fusion proteins generally have to be expressed in high levels. Furthermore, verification, whether changes in fluorescence emission are caused by energy transfer, requires complicated irreversible photobleaching or fluorescence lifetime imaging techniques (Chen *et al.*, 2003; Periasamy, 2000). However, the instrumental equipment necessary for these techniques is not widely available and FRET requires intensive methodical training. For these reasons reports about FRET-based protein–protein interaction investigations in living cells have remained rare especially in plant science (Immink *et al.*, 2002; Más *et al.*, 2000; Shah *et al.*, 2002; Vermeer *et al.*, 2004).

Alternatively, protein interactions can also be investigated *in vivo* if the protein complex formation can be visualized by the restoration of a detectable activity. In this regard, the principle of intragenic complementation of the *lacZ* locus from *Escherichia coli* was adapted to detect protein interactions (Rossi *et al.*, 1997; Ullmann *et al.*, 1967). In this experimental system the detection of protein–protein interactions by restoration of β-galactosidase activity was enabled by using β-galactosidase fragments, which could associate only when fused to interacting proteins. Similarly, fragments of the dihydrofolate reductase have been used in protein interaction studies based on complementation of protein function (Pelletier *et al.*, 1998). However, these techniques require the application of extrinsic fluorophores to visualize the complex formation.

An alternative experimental approach for the visualization of protein interactions is based on the formation of a fluorescent complex by fragments of the enhanced yellow fluorescent protein (YFP) when brought together by the interaction of two associating partners fused to these fragments. Recently, Kerppola and colleagues (2002) reported a proof-of-concept for such an approach for the investigation of protein interactions in living mammalian cells and designated this technique as bimolecular fluorescence complementation (BiFC). The unique characteristic of the BiFC approach is that the bright intrinsic fluorescence of the bimolecular complex allows direct visualization of the complex formation in living mammalian cells. Moreover, by analyzing the interactions between members of the basic leucine zipper (bZIP) and Rel transcription factor families, the BiFC approach provided direct evidence of the intracellular locations where the protein association occurs (Hu *et al.*, 2002). The application of the BiFC approach has recently been extended to the investigation of the interaction pattern and intracellular localization of G-protein complexes in mammalian cells and *Dictyostelium discoideum* (Hynes *et al.*, 2004) and to the visualization of 1-aminocyclopropane-1-carboxylase synthase heterodimer formation in *E. coli* (Tsuchisaka and Theologis, 2004). Furthermore, by introducing a large number of different GFP variants the technique was extended to multicolor BiFC, which allows the direct visualization of multiple protein interactions within the same cell (Grinberg *et al.*, 2004; Hu and Kerppola, 2003).

In this report we describe the generation of several sets of plant-compatible BiFC vectors. We used these vectors for investigating the interaction of plant nuclear and cytoplasmic proteins in different plant systems. Our study attests the general applicability of the BiFC technique and that this assay represents an efficient and convenient tool to investigate protein–protein interactions in living plant cells.

Results

Generation of plant-compatible BiFC transformation vectors

To develop the BiFC technology for the visualization of protein–protein interactions in living plant cells, we constructed four pairs of vectors (Figure 1; for further details see Experimental procedures and Supplementary material). These vectors have been designated *pSPYNE* and *pSPYCE* (for split YFP N-terminal/C-terminal fragment expression) respectively. Each vector pair enables the expression of proteins of interest fused either to the N-terminal 155 amino acids (YFP^N) or to the C-terminal 86 amino acids of YFP (YFP^C; Hu *et al.*, 2002). Moreover the plasmids contain either a c-myc (*pSPYNE*) or HA (*pSPYCE*) affinity tag for detection of fusion protein expression in cell extracts (Figure 1). The binary *pSPYNE-KAN* and *pSPYCE-BAR* vectors enable the expression of YFP fragment-fused genomic DNA or of YFP-fragment constructs driven by any promoter of interest (Figure 1). Strong and constitutive expression of fusion proteins in plant cells is ensured by the binary *pSPYNE-35S* and *pSPYCE-35S* plasmids which contain the *35S* promoter of the cauliflower mosaic virus. For selection of transgenic plants *pSPYNE-KAN* and *pSPYNE-35S* carry a *nos* promoter-driven kanamycin resistance gene (*nptII*), whereas *pSPYCE-BAR* and *pSPYCE-35S* harbor the *bar* gene conferring

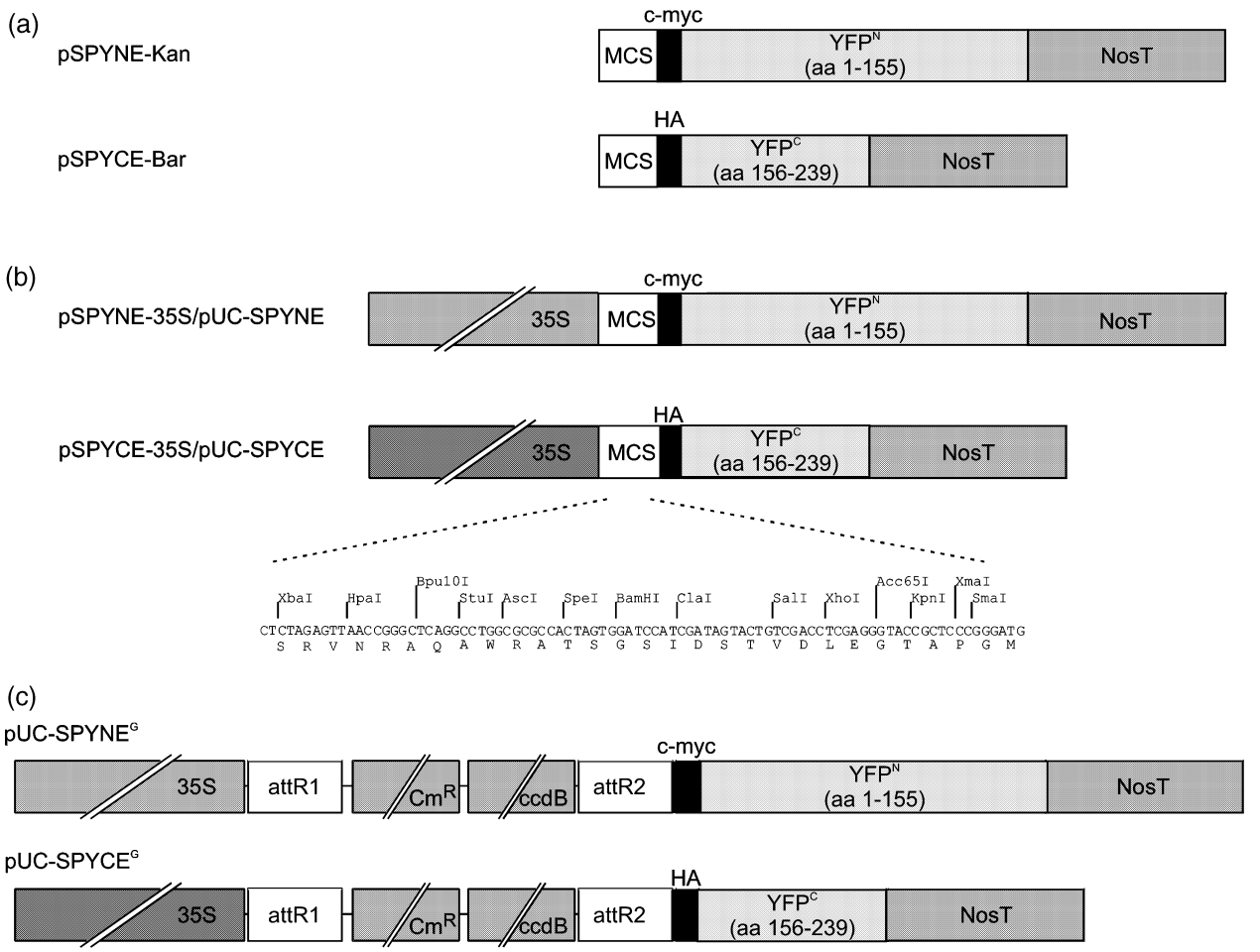

Figure 1. Schematic representation of plant-compatible BiFC vectors.
(a) pSPYNE-Kan and pSPYCE-Bar.
(b) pSPYNE-35S/pUC-SPYNE and pSPYCE-35S/pUC-SPYCE.
(c) pUC-SPYNE^G and pUC-SPYCE^G.
Details of the plasmid construction and vector back bones are given in Experimental procedures and in Figures S1 and S2. c-myc, c-myc affinity tag; HA, hemagglutinin affinity tag; MCS, multi-cloning site; 35S, 35S promoter of the cauliflower mosaic virus; NosT, terminator of the *Nos* gene; YFP^N, N-terminal fragment of YFP reaching from amino acid (aa) 1 to 155; YFP^C, C-terminal fragment of YFP reaching from amino acid 156 to 239; attR1-Cm^R-ccdB-attR2, Gateway conversion cassette.

insensitivity to the herbicide glufosinate (Figure 1). In addition, we generated two additional sets of vectors based on *pUC19* that are specially designed for transient plant cell transformation approaches. *pUC-SPYNE* and *pUC-SPYCE* contain the entire expression cassette of *pSPYNE-35S* or *pSPYCE-35S*, respectively, and harbor a more variable multi-cloning site (MCS) (Figure 1). Furthermore, in a second set the entire MCSs of *pUC-SPYNE* and *pUC-SPYCE* were replaced by the Gateway conversion cassette providing the *attR1* and *attR2* recombination sites for use with the Gateway cloning system (*pUC-SPYNE^G*, *pUC-SPYCE^G*, Figure 1).

BiFC analysis of Arabidopsis *nuclear bZIP63*

To address the feasibility of BiFC for visualization of protein–protein interaction in living plant cells we first choose a member of the *Arabidopsis* bZIP factor family (bZIP63, AGI: At5g28770) as a model protein. bZIP63 belongs to subfamily C of *Arabidopsis* bZIP factors (Jakoby *et al.*, 2002). This transcription factor binds to promoter elements containing the CACGTG or GACGTC sequence *in vitro* and is localized to the nucleus of plant cells (Näke, 2001). Moreover, bZIP transcription factors are known to form homodimers and heterodimers via the C-terminal leucine zipper domain (Siberil *et al.*, 2001).

To first investigate the interaction potential of bZIP63 by an independent experimental approach, we performed an interaction analysis in the yeast two-hybrid system. As shown in Figure 2, bZIP63 formed homodimers *in vivo* as demonstrated by the growth of transformants on interaction selective medium and induction of β-galactosidase reporter activity above background level. To corroborate that the

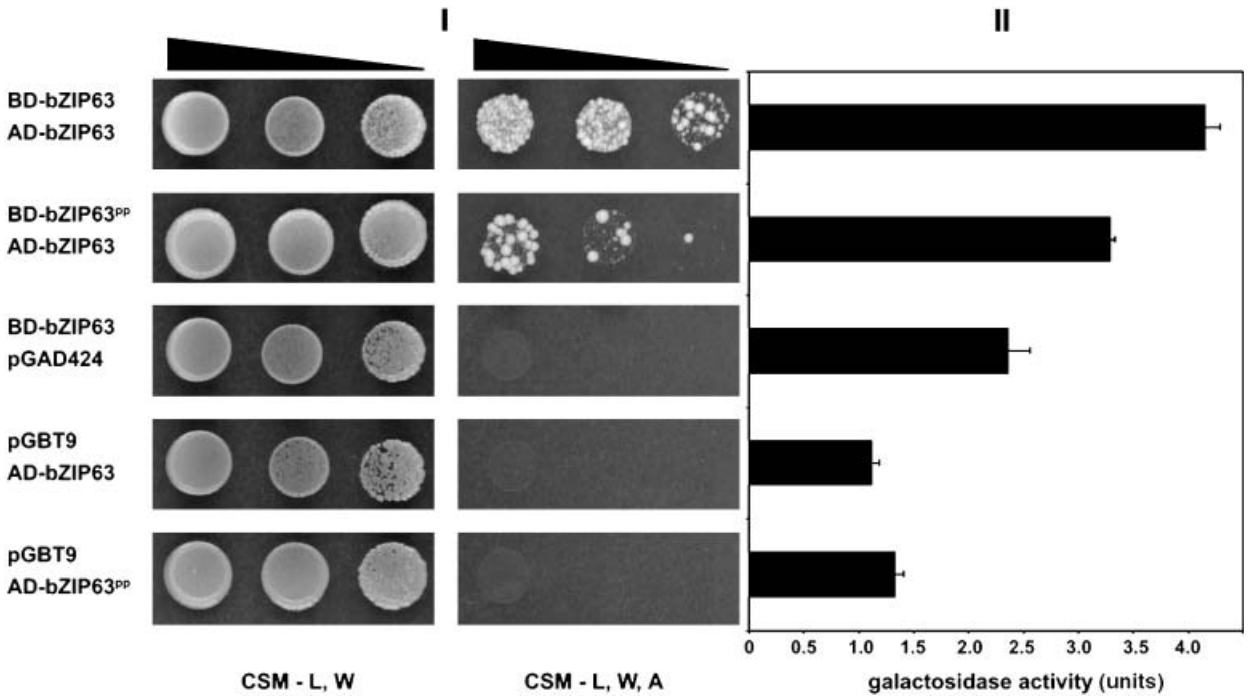

Figure 2. Homodimerization of bZIP63 and bZIP63^{PP} in yeast.
The indicated Gal4 DNA-binding domain (BD) and activation domain (AD) constructs were transformed into yeast strain PJ69-4A. Transformants were assayed for the activity of protein–protein interaction reporting genes either by growth in decreasing densities (narrowing triangle) on selective medium (I: CSM-L,W,A) or determination of β-galactosidase activity (II). CSM-L,W (I) depicts a dilution series on non-selective control plates. bZIP63^{PP} represents a mutated version of bZIP63 in which Leu188 and Leu195 have been mutated to Pro.

homodimer formation is mediated by the leucine zipper we introduced two point mutations in the *bZIP63* sequence which changed Leu188 and Leu195 into Pro. Leu188 and Leu195 are the first two hydrophobic amino acids in the C-terminal zipper-forming amphipathic α-helix of the bZIP63 monomers. Therefore, conversion of these positions into prolines is likely to interfere with the dimerization potential of the protein (Siberil *et al.*, 2001). The combination of wild type bZIP63 with the mutated version (bZIP63^{PP}) reduced expression of the reporter genes (Figure 2). It is noteworthy that in yeast mutation of Leu188 and Leu195 to proline does not completely abolish homodimerization of bZIP63 (Figure 2). In summary, these data indicate that the leucine zipper domain is predominantly responsible for bZIP homodimer formation in yeast.

We next attempted the direct visualization of homodimerization in living plant cells. To this end, we transiently transfected *Arabidopsis* cell culture protoplasts with various *pUC-SPYNE*/*pUC-SPYCE* constructs of *bZIP63* and, in addition to microscopic analysis, quantified the fluorescence intensity. Whereas cells transfected with single plasmids and any combination with empty vectors produced no or only background fluorescence, a strong signal was observed when bZIP63-YFP^{N} was co-expressed with bZIP63-YFP^{C} (Figure 3a,b). Significantly weaker fluorescence signals were observed when combinations of *bZIP63^{PP}* with wild type *bZIP63* were transfected, thereby reflecting reduction in homodimerization by these mutations (Figure 3a,b). Generally the number of BiFC signal-emitting protoplasts was about the half compared with cells expressing full-length GFP fusion proteins. This difference corresponds to the reduced efficiency when more than one construct is used for transfection.

To test the functionality of the binary BiFC vectors *in planta*, the wild type *bZIP63* and *bZIP63^{PP}* cDNAs were cloned into *pSPYNE-35S* and *pSPYCE-35S,* respectively. The constructs were delivered into leaf cells of tobacco (*Nicotiana benthamiana*) by *Agrobacterium* infiltration (Voinnet *et al.*, 2003; Witte *et al.*, 2004). Similar to the situation in *Arabidopsis* protoplasts strong YFP fluorescence was observed when wild type combinations of bZIP63 were expressed (Figure 4a, panels I, II). Pairwise expression of bZIP63 and bZIP63^{PP}, bZIP63^{PP} alone or in combination with the YFP fragments induced no or only weak fluorescence signals (Figure 4a, panels I, II and data not shown). Using HA- and c-myc-tag-specific antibodies the expression of all fusion proteins in tobacco cells was demonstrated (Figure 4a, panel III). Notably, we observed that the transformation efficiency of *Agrobacterium*-infiltrated tobacco cells strongly depends on the constructs used. For instance, whereas 80% of epidermal cells which have been infiltrated with bZIP63-YFP^{N} and bZIP63-YFP^{C}-carrying *Agrobacteria*

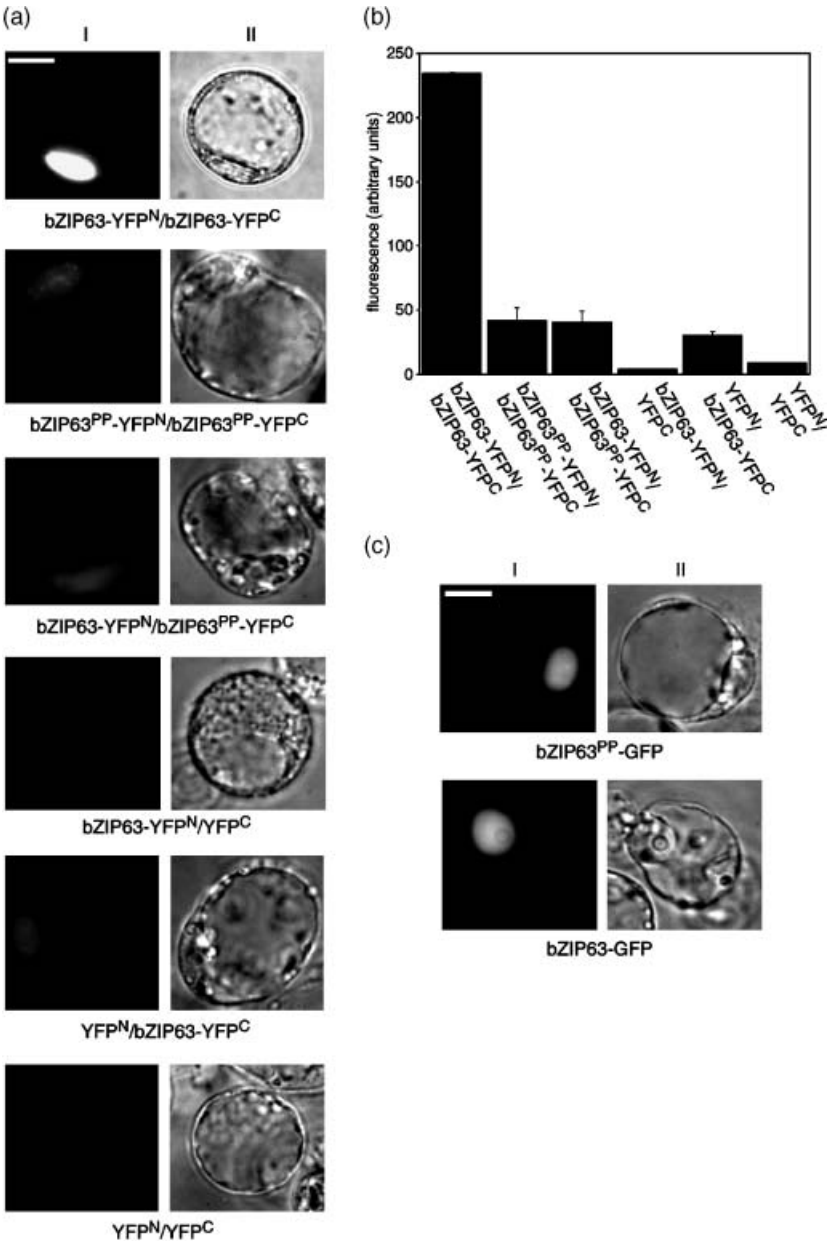

Figure 3. BiFC visualization of bZIP63 dimerization in transiently transfected *Arabidopsis thaliana* cell culture protoplasts.
(a) Epifluorescence (I) and bright field images (II) images of *Arabidopsis* cell culture protoplasts co-transfected with constructs encoding the indicated fusion proteins.
(b) Quantification of fluorescence intensities in transiently transfected *Arabidopsis* cell culture protoplasts. Fluorescence intensity (arbitrary units) was determined using the Metamorph software. The mean and standard deviation of three independent measurements are shown.
(c) bZIP63-GFP and bZIP63^{PP}-GFP are localized to the nucleus. Epifluorescence (I) and bright field (II) images of protoplasts transfected with constructs expressing the indicated fusion proteins. Scale bars, 20 μm.

showed BiFC-induced fluorescence, LSD1 homodimer formation (see Figure 7) was observed in only 20% of the cells.

In transfected *Arabidopsis* protoplasts and infiltrated tobacco leaves the homodimerization-induced YFP fluorescence appeared exclusively inside the nucleus which is in agreement with the observation that bZIP63-GFP and bZIP63^{PP}-GFP are nuclear proteins (Figures 3c and 4b).

BiFC analysis of proteins in the cytoplasm of plant cells

To further extend the applicability of BiFC beyond bZIP transcription factors we analyzed a 14-3-3 protein (isoform T14-3c from *N. tabacum*; GenBank: NTU91724) and the zinc finger protein LSD1 from *Arabidopsis thaliana* (Dietrich *et al.*, 1997) by BiFC analyses in *Arabidopsis* protoplasts and *Agrobacterium*-infiltrated tobacco leaves respectively.

14-3-3 proteins form a conserved family of eukaryotic polypeptides that were the first signaling molecules identified as discrete phosphoserine/phosphothreonine-binding modules. They associate to homodimers or heterodimers with a saddle-shaped structure, with each monomer forming an extended groove that allows binding of the phosphorylated sequence motif (Rittinger *et al.*, 1999; Würtele *et al.*, 2003). Dimerization of 14-3-3 proteins occurs via their N-terminal region. Accordingly, yeast two-hybrid analyses revealed that an N-terminally truncated version of T14-3c is

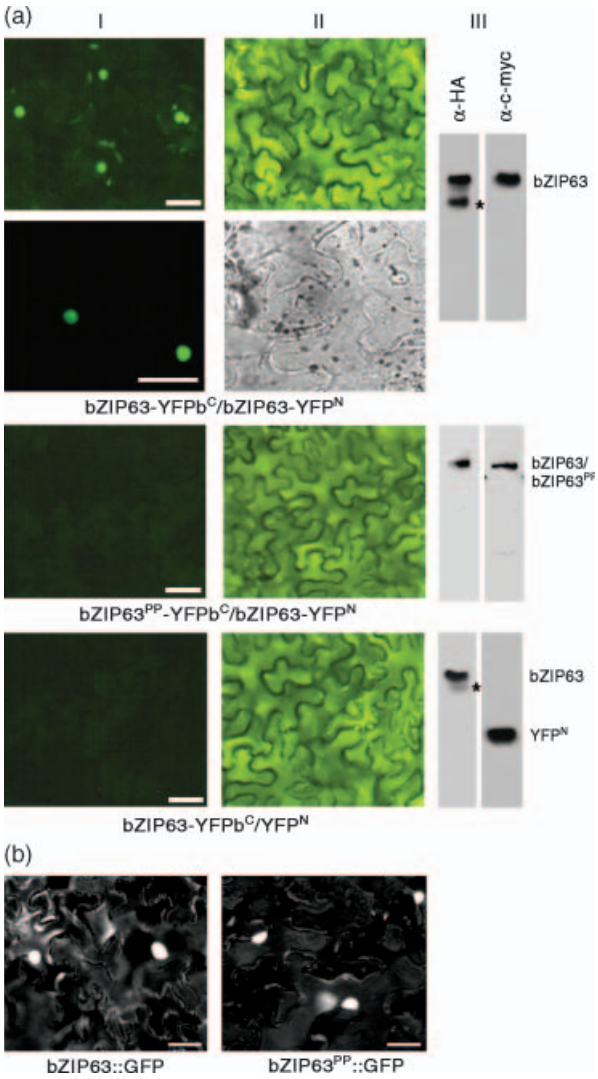

Figure 4. BiFC visualization of bZIP63 dimerization in *Agrobacterium*-infiltrated tobacco (*Nicotiana benthamiana*) leaves.
(a) Epifluorescence (I) and bright field (II) images of epidermal leaf cells infiltrated with a mixture of *Agrobacterium* suspensions harboring constructs encoding the indicated fusion proteins. In addition, the second panel from above shows a confocal image of BiFC-induced bZIP63 dimerization. For technical details of infiltration see Experimental procedures. The expression of the proteins (III) is demonstrated by immunodetection with anti-HA (α-HA) antibodies for YFP^{C} fusions and anti-c-myc (α-c-myc) for YFP^{N} fusions. *, degradation product.
(b) bZIP63-GFP and bZIP63^{PP}-GFP are both localized to the nucleus of plant cells. Epifluorescence images of *Agrobacterium*-infiltrated tobacco (*N. benthamiana*) epidermal cells are shown.
Scale bars, 50 μm.

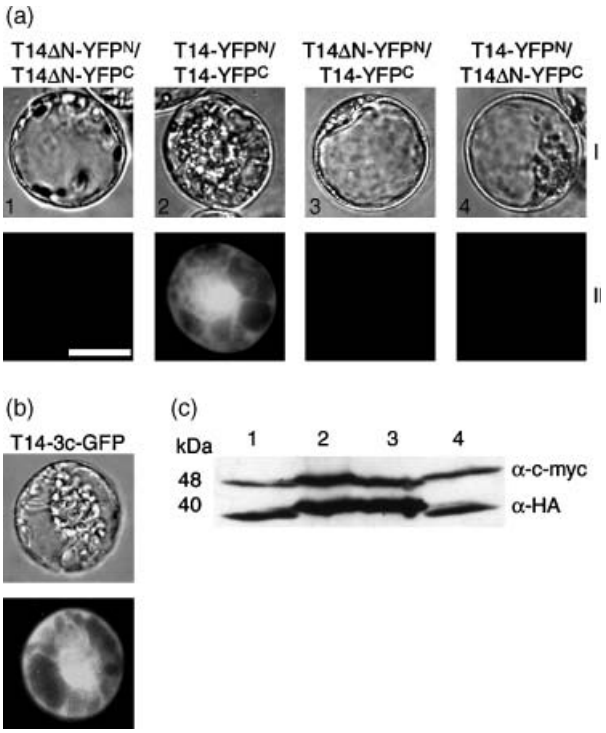

Figure 5. The tobacco 14-3-3 protein T14-3c interacts in *Arabidopsis* cell culture protoplasts.
(a) Bright field (I) and epifluorescence (II) images of *Arabidopsis* cell culture protoplasts co-transfected with constructs encoding the indicated fusion proteins.
(b) T14-3c-GFP is localized to the cytoplasm and nucleus. Bright field (I) and epifluorescence (II) images of protoplasts transfected with a construct expressing T14-3c-GFP are depicted.
(c) Demonstration of protein expression by immunodetection with anti-HA (α-HA) antibodies for YFP^{C} fusions and anti-c-myc (α-c-myc) for YFP^{N} fusions. Extracts from protoplasts co-transfected with the constructs indicated in (a) are shown (lanes 1–4).
Scale bars, 20 μm.

no longer able to homodimerize (Jaspert and Oecking, 2002). For BiFC studies the cDNAs encoding wild type T14-3c (T14) and the mutant version (T14ΔN) were cloned into *pUC-SPYNE* and *pUC-SPYCE* or *pSPYNE-35S* and *pSPYCE-35S*, respectively, and transformed into either *Arabidopsis* protoplasts or tobacco leaf cells. Upon co-expression of T14-YFP^{N} and T14-YFP^{C}, strong YFP fluorescence was detected throughout the cytoplasm and the nucleus in both systems indicating that homodimerization occurs in both compartments (Figures 5a and 6a). In transformed epidermal cells of tobacco the cytoplasmic fluorescence typically appears as a thin area between the cell wall and the turgescent vacuole. Plasmolysis of the cells by treatment with 500 mM mannitol demonstrated the localization of the BiFC signal in the cytoplasm (data not shown). Importantly, the localization of homodimer formation corresponds to the subcellular distribution of T14-3c, when expressed as GFP fusion in protoplasts or tobacco leaf cells under the control of the 35S promoter (Figures 5b and 6b). In contrast, expression of neither the N-terminal truncated form T14ΔN fused to the YFP fragments nor any combination of wild type with the truncated version resulted in a YFP signal (Figures 5a and 6a). Western blot analysis confirmed that the expression of

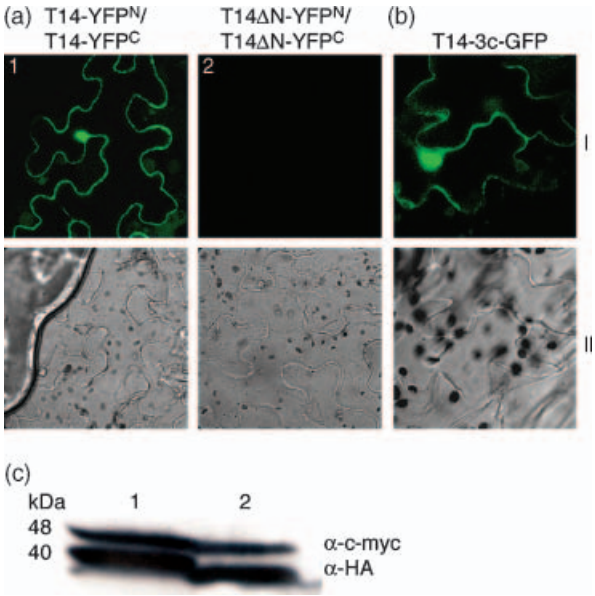

Figure 6. BiFC visualization of T14-3c dimerization in tobacco leaves.
(a) Confocal (I) and bright field (II) images of epidermal leaf cells from *Nicotiana benthamiana* infiltrated with a mixture of *Agrobacterium* suspensions harboring constructs encoding the indicated fusion proteins. For technical details of infiltration see Experimental procedures.
(b) T14-3c-GFP is localized to the cytoplasm and nucleus. Confocal (I) and bright field (II) images of stably transformed *N. tabacum* epidermal cells are depicted.
(c) Demonstration of protein expression by immunodetection with anti-HA (α-HA) antibodies for YFP^C fusions and anti-c-myc (α-c-myc) for YFP^N fusions. Extracts from tissue co-transformed with constructs co-expressing either T14-YFP^N and T14-YFP^C (lane 1) or T14ΔN-YFP^N and T14ΔN-YFP^C (lane 2) are shown.

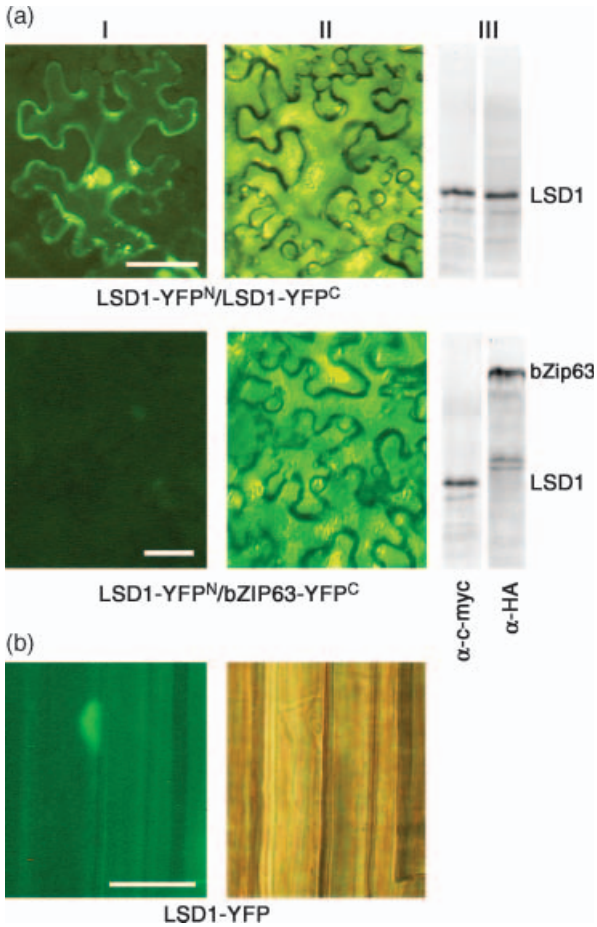

Figure 7. LSD1 forms homodimers *in planta* but does not interact with bZIP63.
(a) Epifluorescence (I) and bright field (II) images of epidermal leaf cells infiltrated with a mixture of *Agrobacterium* suspensions harboring constructs encoding the indicated fusion proteins. For technical details of infiltration see Experimental procedures. The expression of the proteins (III) is demonstrated by immunodetection with anti-HA (α-HA) antibodies for YFP^C fusions and anti-c-myc (α-c-myc) for YFP^N fusions.
(b) LSD1-YFP is localized to the nucleus and cytoplasm of *Arabidopsis* cells. Epifluorescence (I) and bright field (II) images of hypocotyl cells from transgenic *Arabidopsis* plants which express LSD1-YFP are depicted.
Scale bars, 50 μm.

the non-interacting T14-3c fusion proteins was comparable with the expression of the interacting form of T14-3c (Figures 5c and 6c).

LSD1 is a small zinc finger protein that forms homodimers *in vivo* and functions as a negative regulator of programmed cell death in plants (Dietrich *et al.*, 1997; Epple *et al.*, 2003). As observed for the T14-3c homodimer, co-expression of LSD1-YFP^N and LSD1-YFP^C induced strong fluorescence in the cytoplasm and the nucleus of infiltrated tobacco cells, whereas control pairs gave no or only a very weak YFP signal (Figure 7a and data not shown). Again, the location of LSD1 homodimer formation is identical to the localization of LSD1-YFP when expressed under the control of the 35S promoter in transgenic *Arabidopsis* plants (Figure 7b). To test the specificity of LSD1 protein association, we analyzed the interaction of bZIP63 and LSD1 in co-transformed tobacco leaf cells. This protein pair was chosen because in the yeast two-hybrid system bZIP63 does not interact with LSD1 (Näke, 2001). As shown in Figure 7, co-expression of bZIP63 and LSD1 in any combination revealed no fluorescence, although the fusion proteins were expressed.

Discussion

In this report we establish BiFC as a very efficient technology for the analysis of protein–protein interactions in living plants cells. The vectors described are readily suitable for BiFC analyses in *Arabidopsis* protoplasts and *Agrobacterium*-infiltrated tobacco leaves. They also allow determination of protein expression levels by Western blot analysis. The binary BiFC vectors will also enable interaction and protein complex formation studies in transgenic plants. However, at high expression levels the free YFP fragments sometimes tend to associate non-specifically, thereby

generating background fluorescence (Figure 3a,b). This problem can be circumvented, when a non-interacting fusion protein is used in the control experiments as exemplarily shown for the T14ΔN and bZIP63/LSD1 pairs, or if the expression level is reduced by the use of a less active promoter.

Our BiFC analyses of interactions among bZIP63, T14-3c and LSD1 in living plant cells illustrate several significant advantages of this technique (Hu *et al.*, 2002). (i) Protein interactions using BiFC are visualized in the normal environment of the plant cell. Several restrictions inherent to interaction approaches in heterologous systems (e.g. yeast), as for instance missing plant-specific post-translational protein modifications or incorrect subcellular localization, are overcome by BiFC. From a technical point of view the detection of BiFC-generated interactions does not require accessibility of the protein complex to extrinsic fluorophores and does not require the instrumental equipment necessary for FRET including subsequent complex data processing. (ii) Compared with published FRET data (Immink *et al.*, 2002; Más *et al.*, 2000; Shah *et al.*, 2002; Vermeer *et al.*, 2004) the BiFC signals observed in our study using the strong viral 35S promoter for the expression of the fusion proteins appear to be very intense. Comparison of the microscopic exposure times suggest that for a given protein interaction the BiFC fluorescence intensity can reach about 30% of the signal intensity of the corresponding full-length GFP. From these data we conclude that BiFC is very sensitive and may allow the detection of interactions when the proteins are expressed at lower levels under the control of native promoters. As demonstrated by our study and recent reports (Grinberg *et al.*, 2004; Hynes *et al.*, 2004) BiFC-generated fluorescence signals can also be quantified. Thus, the ability of a protein to form different complexes with different interaction partners can be quantitatively determined at the cellular or even the subcellular level (Grinberg *et al.*, 2004). (iii) The most appealing advantage of BiFC is that protein interaction occurs in the genuine compartment of the proteins examined. *Arabidopsis* bZIP63 is a nuclear transcriptional regulator and homodimer formation is exclusively detected by BiFC inside the nucleus. When expressed under the control of the viral 35S promoter, tobacco T14-3c and *Arabidopsis* LSD1 accumulate in the cytoplasm and in the nucleus. Again, BiFC dimer formation strictly coincides with observed localization in these compartments. This should enable the identification of the subcellular distribution of interaction between regulatory proteins like transcription factors and signaling components and may immediately provide information about the functional role of the association. For instance, in mammalian HEK-293 cells BiFC analyses revealed that the different β subunits of G proteins direct the corresponding βγ signaling complexes to alternative subcellular locations (Hynes *et al.*, 2004). Furthermore in, mammalian cell lines using BiFC Kerppola and colleagues demonstrated that the cytoplasmic transcription factor Mad4 was recruited to the nucleus through dimerization with Max (Grinberg *et al.*, 2004) and were able to identify the intramolecular region responsible for the differential intracellular distribution of ATF2/Jun heterodimers (Hu *et al.*, 2002). (iv) Formation of the BiFC protein complex occurs through a multistep pathway *in vitro* and very likely *in vivo* (Hu *et al.*, 2002). The initial steps are mediated by contacts between the proteins fused to the YFP fragments and are reversible. At this initial state complex formation can be competed by alternative interaction partners. Afterwards the initial complex is stabilized by the association of YFP fragments and further exchange of protein components is inhibited (Hu *et al.*, 2002). Therefore, the kinetics of BiFC formation allows the detection of weak and transient protein complexes *in vivo* but has the disadvantage that shifts in the equilibrium between putative alternative complexes may hardly be detectable after initial formation. However, we expect that the dynamics of BiFC protein complex formation is still maintained or can be still modified by the cellular protein folding and degradation machinery. (v) The structural background of protein complex formation can likewise be investigated by BiFC. For instance, truncation of the N-terminal region of the tobacco T14-3c protein or point mutations within the C-terminal leucine zipper of *Arabidopsis* bZIP63 identified these domains to be responsible for homodimerization in plant cells. (vi) In perspective, the BiFC approach enables the identification of signals that induce the formation of protein complexes or modulate their intracellular distribution *in planta*. Accordingly, it has been shown that a BiFC complex consisting of the ATF2-Jun heterodimer is translocated into the nucleus of mammalian COS cells after expression of the stress-activated p38 SAPK protein kinase (van Dam *et al.*, 1995; Hu *et al.*, 2002).

From the studies in mammalian cells using a set of different Jun-YFP^N and Fos-YFP^C fusion polypeptides, it has been estimated that fluorescence complementation may occur when the YFP fragments are separated by an average distance of greater than 100 Å (Hu *et al.*, 2002). A prerequisite for complementation over long distance is sufficient flexibility of the protein backbone, to which the fragments are fused. This then allows association of the YFP fragments to stabilize the initial BiFC complex. Therefore, the dynamics of BiFC complex formation in combination with sufficient complementation over long distance may enable the identification of novel protein interactions in plant cells by genetic screens based, for example, on high-efficiency protoplast transformation accompanied by fluorescence-activated cell sorting (Birnbaum *et al.*, 2003; Galbraith, 2004). Furthermore, by generating large populations of transgenic plants expressing distinct YFP^N or YFP^C fusion proteins, interaction screens can also be performed on whole plant level by crossing individual lines.

Experimental procedures

Generation of plant BiFC vectors and plant expression constructs

Molecular techniques were performed using standard protocols according to Sambrook and Russell (2001) and Kudla *et al.* (1999). To generate the vector system for BiFC analysis we amplified fragments of eYFP coding for the N-terminal 155 and C-terminal 84 aa, thereby introducing *Xma*I and *Sac*I restriction sites for cloning and sequences for c-myc and HA affinity tags respectively. The PCR products were cloned into the *Xma*I and *Sac*I sites of *pGPTVII.Kan* and *pGPTVII.Bar* resulting in *pSPYNE-Kan* and *pSPYCE-Bar*. The same PCR products were cloned via *Xma*I/*Sac*I into *pGPTVII.GFP.Kan* and *pGPTVII.GFP.Bar* resulting in *pSPYNE-35S* and *pSPYCE-35S* (for *pGPTVII* vector series see Figure S1 and S2). The pUC19 derivatives were generated by replacing the entire expression cassette of psmGFP4 with the expression cassettes of *pSPYNE-35S* and *pSPYCE-35S* via *Hin*dIII and *Eco*RI, resulting in *pUC-SPYNE* and *pUC-SPYCE*. These vectors were further modified to obtain the Gateway-compatible vectors *pUC-SPYNE*^{G} and *pUC-SPYCE*^{G}. To this end, the entire multiple cloning site of *pUC-SPYNE* and *pUC-SPYCE* was excised with *Xba*I and *Sma*I, and after blunting replaced with the Gateway vector conversion cassette B (Invitrogen, Carlsbad, CA, USA). The cDNA regions encoding the proteins and polypeptides investigated in this study were amplified from plasmid templates containing the corresponding cDNA by PCR using gene-specific primers and cloned into *pGEM-T* (Promega, Madison. WI, USA) or pBluescript (Stratagene, La Jolla, CA, USA) respectively. Site-directed mutagenesis of the *bZIP63* cDNA was carried out using the Quick-Change Site-directed Mutagenesis Kit according to the manufacturer's protocol (Stratagene). Primer sequences can be obtained upon request. PCR products were verified by sequencing and subsequently cloned into each of the BiFC vectors, *pUC-SPYNE/pSPYNE-35S* and *pUC-SPYCE/pSPYCE-35S* by using the *Bam*HI/*Sma*I (*T14-3c*, N-terminal truncated *14-3c*), *Bam*HI/*Xho*I (*bZIP63*, *bZIP63*^{PP}) or *Sma*I/*Bam*HI (*LSD1*) restriction sites. For the generation of GFP fusion constructs, the coding region of *T14-3c* was cloned via *Kpn*I/*Bam*HI into *pCF203*, those of *bZIP63* and *bZIP63*^{PP} via *Bam*HI/*Xho*I into *pGPTVII-GFP*, and that of *LSD1* via *Bam*HI/*Sma*I into *pPCVB-YFP*.

Protoplast transfection, plant transformation, microscopic techniques, and quantification of fluorescence intensity

Protoplasts were generated from 1-week-old *Arabidopsis* Col-0 suspension cell culture (Liu *et al.*, 2003). The cells were collected by centrifugation at 400 ***g*** for 5 min and the pellet was washed with 25 ml of cell wall digestion buffer lacking the digestion enzymes. Protoplasts were prepared and transformed according to the protocols of Merkle *et al.* (1996) and Negrutiu *et al.* (1987). Protoplasts were assayed for fluorescence 12–18 h after transfection. For infiltration of *N. benthamiana*, the *Agrobacterium tumefaciens* strain C58C1 carrying the pCH32 helper plasmid was infiltrated into the abaxial air space of 2–4-week-old plants as described (Voinnet *et al.*, 2003; Witte *et al.*, 2004). The p19 protein of tomato bushy stunt virus was used to suppress gene silencing. Co-infiltration of *Agrobacterium* strains containing the BiFC constructs and the p19 silencing plasmid was carried out at OD_{600} of 0.7:0.7:1.0. Epidermal cell layers of tobacco leaves were assayed for fluorescence 1–2 days after infiltration. Stable transformation of *N. tabacum* SNN and *Arabidopsis thaliana* (Col-0) with *Agrobacterium* was carried out as described previously (Bechthold *et al.*, 1993; Martin *et al.*, 1993). Microscopic techniques were performed according to Kircher *et al.* (1999) and images were processed using the Adobe Photoshop software package. Quantification of fluorescence signal intensity was carried out using the Metamorph software package (Universal Imaging Corporation Downington, PA, USA).

Yeast two-hybrid interaction assays, protein extraction and assay, SDS-PAGE, Western blot and immunodetection

Yeast two-hybrid interaction tests (in strain PJ69-4A) including growth and quantitative β-galactosidase reporter gene assays were performed as described previously (Albrecht *et al.*, 2001; Lohrmann *et al.*, 2001). Transfected protoplasts and *Agrobacterium*-infiltrated tobacco leaf discs were extracted under denaturing conditions using boiling SDS-sample buffer supplemented with 4 M urea (Harter *et al.*, 1993). Protein assay, SDS-PAGE, Western blot transfer and immunodetection using HA- (Roche, Basel, Switzerland) and c-myc-specific (Sigma, St. Louis, MO, USA) antibodies has been described elsewhere (Harter *et al.*, 1993).

Acknowledgements

We thank D. Baulcombe and T. Romeis for the *Agrobacterium* strain C58C1, and the p19 construct and C. Frankhauser for the pCF203 plasmid. We are also very thankful to G. Freymark who introduced to us the *Agrobacterium* infiltration technique, to G. Fiene, C. Brancato, D. Kreuder, L. Rößner and C. Spitzer for excellent technical assistance and to D. Wanke for help in image processing. This work was supported by grants of the Deutsche Forschungsgemeinschaft to C.O. (SFB 446), K.H. (SFB 635, HA 2146/3-2, 5-1) and to J.K. (931/4-1, 4-2).

Note added in proof

The usefulness of BiFC for in planta-protein interaction studies is also presented in the paper by Bracha-Drori *et al.* (2004), in this issue.

Supplementary material

The following material is available from http://www.blackwellpublishing.com/products/journals/suppmat/TPJ/TPJ2219/TPJ2219sm.htm.

Figure S1. (a) Schematic depiction of the series of pGPTVII vectors (kan, bar, hyg). Unique restriction sites are given in bold letter, others in italics.

(b) Multiple cloning site of the pGPTVII vector series. Unique restriction sites (above the nucleotide sequence) are illustrated in normal letters. Restriction sites marked with * are not unique in pGPTVII.Bar.

Figure S2. (a) Schematic depiction of the series of pGPTVII.GFP vectors (kan, bar, hyg). Unique restriction sites are given in bold letters, others in italics.

(b) Multiple cloning site of pGPTVII. GFP vectors. Below the nucleotide sequence the amino acid sequence of the multiple cloning is illustrated, which is in frame to the first methionine of GFP (underlined). Unique restriction sites (above the nucleotide sequence) are illustrated in normal letters, others in italics. Restriction sites marked with * are not unique in pGPTVII.GFP.Bar. In pGPTVII.CFP and pGPTVII.YFP the GFP was replaced by the respective fluorescent marker proteins.

References

Albrecht, V., Ritz, O., Linder, S., Harter, K. and Kudla, J. (2001) The NAF domain defines a novel protein–protein interaction module conserved in Ca^{2+}-regulated kinases. *EMBO J.* **20**, 1051–1063.

Bechthold, N., Ellis, J. and Pelletier, G. (1993) In planta *Agrobacterium*-mediated gene transfer by infiltration of adult *Arabidopsis thaliana* plants. *CR. Acad. Sci. Paris Life Sci.* **316**, 1194–1199.

Birnbaum, K., Shasha, D.E., Wang, J.Y., Jung, J.W., Lambert, G.M., Galbraith, D.W. and Benfey, P.N. (2003) A gene expression map of the *Arabidopsis* root. *Science*, **302**, 1956–1960.

Chen, Y., Mills, J.D. and Periasamy, A. (2003) Protein localization in living cells and tissues using FRET and FLIM. *Differentiation*, **71**, 528–541.

van Dam, H., Wilhelm, D., Herr, I., Steffen, A., Herrlich, P. and Angel, P. (1995) ATF-2 is preferentially activated by stress-activated protein kinases to mediate c-jun induction in response to genotoxic agents. *EMBO J*, **14**, 1798–1811.

Dietrich, R.A., Richberg, M.H., Schmidt, R., Dean, C. and Dangl, J.L. (1997) A novel zinc finger protein is encoded by the *Arabidopsis* LDS1 gene and functions as negative regulator of plant cell death. *Cell*, **88**, 685–694.

Epple, P., Mack, A.A., Morris, V.R.F. and Dangl, J.L. (2003) Antagonistic control of oxidative cell death in *Arabidopsis* by two related, plant-specific zinc finger proteins. *Proc. Natl Acad. Sci. USA*, **100**, 6831–6836.

Field, S. and Song, O.K. (1989) A novel genetic system to detect protein–protein interactions. *Nature*, **340**, 245–246.

Galbraith, D.W. (2004) Cytometry and plant sciences: a personal retrospective. *Cytometry*, **58A**, 37–44.

Grinberg, A.V., Hu, C.-D. and Kerppola, T.K. (2004) Visualization of Myc/Max/Mad family dimers and the competition for dimerization in living cells. *Mol. Cell. Biol.* **24**, 4294–4308.

Harter, K., Talke-Messerer, C., Barz, W. and Schäfer, E. (1993) Light- and sucrose-dependent gene expression in photomixotrophic cell suspension cultures and protoplasts of rape (*Brassica napus* L.). *Plant J.* **4**, 507–516.

Hu, C.-D. and Kerppola, T.K. (2003) Simultaneous visualization of multiple protein interactions in living cells using multicolour fluorescence complementation analysis. *Nat. Biotechnol.* **21**, 539–545.

Hu, C.-D., Chinenov, Y. and Kerppola, T.K. (2002) Visualization of interactions among bZIP and Rel family proteins in living cells using bimolecular fluorescence complementation. *Mol. Cell*, **9**, 789–798.

Hynes, T.R., Tang, L., Mervine, S.M., Sabo, J.L., Yost, E.A., Devreotes, P.N. and Berlot, C.H. (2004) Visualization of G protein $\beta\gamma$ dimmers using bimolecular fluorescence complementation demonstrates roles for both β and γ in subcellular targeting. *J. Biol. Chem.* **279**, 30279–30286.

Immink, R.G.H., Gadella, T.W.J., Jr, Ferrario, S., Busscher, M. and Angenent, G.C. (2002) Analysis of MADS box protein–protein interactions in living plant cells. *Proc. Natl Acad. Sci. USA*, **99**, 2416–2421.

Jakoby, M., Weisshaar, B., Dröge-Laser, W., Vicente-Carbajosa, J., Tiedemann, J., Kroi, T. and Parcey, F. (2002) bZIP transcription factors in *Arabidopsis*. *Trends Plant Sci.* **7**, 106–112.

Jaspert, N. and Oecking, C. (2002) Regulatory 14-3-3 proteins bind the atypical motif within the C-terminus of the plant plasma membrane H^+-ATPase via their typical amphipathic groove. *Planta*, **216**, 136–139.

Kircher, S., Wellmer, F., Nick, P., Rügner, A., Schäfer, E. and Harter, K. (1999) Nuclear import of the parsley bZIP transcription factor CPRF2 is regulated by phytochrome photoreceptors. *J. Cell Biol.* **144**, 201–211.

Kudla, J., Xu, Q., Harter, K., Gruissem, W. and Luan, S. (1999) Genes for calcineurin B-like proteins in *Arabidopsis* are differentially regulated by stress signals. *Proc. Natl Acad. Sci. USA*, **96**, 4718–4723.

Liu, L.H., Ludewig, U., Frommer, W.B. and von Wirén, N. (2003) AtDUR3 encodes a new type of high-affinity urea/H+ symporter in *Arabidopsis*. *Plant Cell*, **15**, 790–800.

Lohrmann, J., Sweere, U., Zabaleta, E., Bäurle, I., Keitel, C., Kozma-Bognar, L., Brennicke, A., Schäfer, E., Kudla, J. and Harter, K. (2001) The response regulator ARR2: a pollen-specific transcription factor involved in the expression of nuclear genes for components of mitochondrial complex I in *Arabidopsis*. *Mol. Genet. Genomics*, **265**, 2–13.

Martin, T., Frommer, W.B., Salanoubat, M. and Willmitzer, L (1993) Expression of an *Arabidopsis* sucrose synthase gene indicates a role in metabolization of sucrose both during phloem loading and in sink organs. *Plant J.* **4**, 367–377.

Más, P., Devlin, P.F., Panda, S. and Kay, S.A. (2000) Functional interaction of phytochrome B and cryptochrome 2. *Nature*, **408**, 207–211.

Merkle, T., Leclerc, D., Marshallsay, C. and Nagy, F. (1996) A plant *in vitro* system for the nuclear import of proteins. *Plant J.* **10**, 1177–1186.

Näke, C. (2001) Charakterisierung von CPRF2-homologen bZIP-Proteinen aus *Arabidopsis thaliana* unter besonderer Berücksichtigung ihrer intrazellulären Verteilung. Inaugural Dissertation. Biologische Fakultät, Universität Freiburg, Germany.

Negrutiu, I., Shillito, R., Potrykus, I., Biasini, G. and Sala, F. (1987) Hybrid genes in the analysis of transformation conditions. *Plant Mol. Biol.* **8**, 363–373.

Pelletier, J.N., Campbell-Valois, F.X. and Michnick, S.W. (1998) Oligomerization domain-directed reassembly of active dihydrofolate reductase from rationally designed fragments. *Proc. Natl Acad. Sci. USA*, **95**, 12141–12146.

Periasamy, A. (2000) Fluorescence resonance energy transfer microscopy: a mini review. *J. Biomed. Opt.* **6**, 287–291.

Rittinger, K., Budman, J., Xu, J., Volinia, S., Cantley, L.C., Smerdon, S.J., Gamblin, S.J. and Yaffe, M.B. (1999) Structural analysis of 14-3-3 phosphopeptide complexes identifies a dual role for the nuclear export signal of 14-3-3 in ligand binding. *Mol. Cell*, **4**, 153–166.

Rossi, F., Charlton, C.A. and Blau, H.M. (1997) Monitoring protein–protein interactions in intact eukaryotic cells by β-galactosidase complementation. *Proc. Natl Acad. Sci. USA*, **94**, 8405–8410.

Sambrook, J. and Russell, D.W. (2001) *Molecular cloning: a laboratory manual*. Cold Spring Harbor, N.Y., Cold Spring Harbor Laboratory Press.

Shah, K., Russinova, E., Gadella, T.W.J., Willemse, J. and de Vries, S.C. (2002) *Arabidopsis* kinase-associated protein phosphatase controls internalization of the somatic embryogenesis receptor kinase 1. *Genes Dev.* **16**, 1707–1720.

Siberil, Y., Doireau, P. and Gantet, P. (2001) Plant bZIP G-box binding factors: modular structure and activation mechanisms. *Eur. J. Biochem.* **268**, 5655–5666.

Stephens, D.J. and Banting, G. (2000) The use of yeast two-hybrid screens in studies of protein:protein interactions involved in trafficking. *Traffic*, **1**, 763–768.

Tsuchisaka, A. and Theologis, A. (2004) Heterodimeric interactions among the 1-amino-cyclopropane-1-carboxylate synthase polypeptides encoded by the *Arabidopsis* gene family. *Proc. Natl Acad. Sci. USA*, **101**, 2275–2280.

Ullmann, A., Jacob, F. and Monod, J. (1967) Characterization by *in vitro* complementation of a peptide corresponding to an operator-proximal segment of the β-galactosidase structural gene of *Escherichia coli*. *J. Mol. Biol.* **24**, 339–343.

Vermeer, J.E.M., Van Munster, E.B., Vischer, N.O. and Gadella, T.W.J., Jr (2004) Probing plasma membrane microdomains in cowpea protoplasts using lapidated GFP-fusion proteins and multimode FRET microscopy. *J. Microsc.* **214**, 190–200.

Voinnet, O., Rivas, S., Mestre, P. and Baulcombe, D. (2003) An enhanced transient expression system in plants based on suppression of gene silencing by the p19 protein of tomato bushy stunt virus. *Plant J.* **33**, 949–956.

Witte, C.-P., Noël, L.D., Gielbert, J., Parker, J.E. and Romeis, T. (2004) Rapid one-step purification from plant material using the eight-amino acid StrepII epitope. *Plant Mol. Biol.* (in press).

Würtele, M., Jelich-Ottmann, C., Wittinghofer, A. and Oecking, C. (2003) Structural view of a fungal toxin acting on a 14-3-3 regulatory complex. *EMBO J.* **22**, 987–994.